Original article

Modelling the profile and internal structure of tree stem.
Application to *Cedrus atlantica* (Manetti)

François Courbet [a,*] and François Houllier [b]

[a] Unité de Recherches forestières méditerranéennes, INRA, avenue Antonio Vivaldi, 84000 Avignon, France
[b] UMR botanique et bioinformatique de l'architecture des plantes, CIRAD, TA40/PS2, boulevard de la Lironde,
34398 Montpellier Cedex 5, France

Abstract – A set of compatible models are established to simulate the profile and internal structure of stems: ring distribution, bark and sapwood profiles. First, models are built tree by tree; they are then generalized by establishing relationships between the estimates of treewise model parameters and the individual tree characteristics. The residuals are examined against the relative height or distance from the apex. Using an independent sample of 4 trees, the observed stem and annual increment profiles are compared to the modelled profiles, firstly using a stem profile model and secondly using a ring profile established previously [10]. Generally, each model proves to be more accurate when used directly to predict the type of profile – stem or increment – for which it has been calibrated. In the lower part of the tree, the ring profile model gives less biased and more accurate estimates of ring width and tree diameter than the stem profile models.

stem profile / growth ring profile / bark profile / sapwood profile / *Cedrus atlantica*

Résumé – Modélisation du profil et de la structure interne de la tige. Application à *Cedrus atlantica* (Manetti). Un ensemble de modèles compatibles entre eux sont établis pour simuler le profil des tiges et leur structure interne : distribution des largeurs de cerne, profils d'écorce et d'aubier. Des modèles sont d'abord construits arbre par arbre puis généralisés par recherche de relations entre les paramètres estimés au niveau arbre et les caractéristiques individuelles des arbres. Les résidus sont ensuite examinés en fonction de la hauteur relative ou de la distance à l'apex. Sur un échantillon indépendant de 4 arbres, les profils de tige et d'accroissement annuels observés sont comparés aux profils modélisés, d'une part par l'utilisation d'un modèle de profil de tige, d'autre part par un modèle de profil de cerne établi antérieurement [10]. De manière générale, chaque modèle se révèle plus précis quand on l'utilise directement pour prédire le type de profil, de tige ou d'accroissement, sur lequel il a été calibré. Dans la partie inférieure de l'arbre, le modèle de profil de cerne donne des estimations moins biaisées et plus précises des largeurs de cerne et du diamètre de l'arbre que les modèles de profil de tige.

profil de tige / profil de cerne / profil d'écorce / profil d'aubier / *Cedrus atlantica*

---

* Correspondence and reprints
Tel. +4 90 13 59 37; Fax +4 90 13 59 59; e-mail: courbet@avignon.inra.fr

1. INTRODUCTION

1.1. Aim and interest of the study

The main aim of this article is to establish a set of compatible models which describe the external form and internal structure of stems, namely stem profile as well as ring, bark and sapwood profiles. These profiles play a key role at the crossroads of tree growth studies and timber quality assessment. They are indeed the direct output of growth processes and provide insight into overall tree functioning [13]. They are also key features for predicting timber quality and optimizing industrial processes [26].

For coniferous trees, there is usually a close and negative relationship between ring width and wood density [2], which itself is very closely linked to the modulus of elasticity [42]. The mechanical resistance of a piece of wood taken from a tree depends greatly on the width and age of its growth rings.

Although it is sometimes used for the heating or artificial drying of wood, bark is often considered as a waste product of no interest to the sawyer. Bark is a compartment rich in nutrients, which is often exported out of the ecosystem with the logs. It is therefore important both from an economic and an ecological point of view, to know the proportion of the tree represented by the bark.

The advantage of knowing the quantity of sapwood is two-fold, firstly in terms of physiology and secondly in terms of its use as a material: (1) with respect to physiology, the sapwood is the main site of upward xylem sap flow. According to the pipe model theory, the amount of sapwood is closely linked to the amount of foliage supplied, expressed either in terms of leaf area or leaf biomass. (2) With respect to wood quality, sapwood, as opposed to heartwood, is considered to be an asset or a drawback depending on what use is made of it. If used for something where aesthetic quality is important or for the manufacturing of paper pulp, the light colour of sapwood is often considered to be an asset and the darker colour of heartwood is considered to be a drawback. Conversely, since sapwood is more sensitive to decay and insect damage than heartwood, the latter is preferred for uses where durability is an advantage (e.g. framing timber, exterior joinery, siding). Furthermore, this natural durability is an asset when applying a more environmentally-friendly ecocertification policy, by reducing the use of chemical impregnation products. In such a context, the heartwood of the Atlas Cedar (*Cedrus atlantica* Manetti), which is naturally decay resistant, represents a real asset.

Atlas cedar, which is relatively drought resistant and very widespread in northern Africa, has been used often for reforestation in southern Europe, above all in France and Italy. Despite the fact that Mediterranean sites are often somewhat unfavourable to forest growth, Atlas cedar stands usually exhibit high productivity levels and provide high quality wood [1]. These models are thus intended to satisfy a real need, concerning a species of great interest, which as yet has been dealt with very little in terms of growth and wood quality modelling.

1.2. Bibliographic review of main profile models

The stem profile models have developed rapidly over the last fifteen years together with the development of non-linear regression techniques. Just as growth models have gradually been replacing yield tables, stem profiles have progressively been taking the place of volume - tables and functions. These profiles are more flexible and make it possible to estimate the volume of a stem cut off at any merchantable height or top diameter limit [6]. Moreover, they have generated considerable progress in the knowledge of tree form and the way it evolves [19, 43].

Numerous functions exist which describe the taper of a tree. Most of them are polynomial, whether segmented [14, 36] or otherwise. Some authors have used trigonometric functions [56], often with less success [52]. Taper equations with variable exponent have recently been undergoing considerable progress [18, 27, 44, 47, 52]. They combine flexibility and simplicity to give quite accurate and robust taper models which are compatible with volume prediction models or with the volume tables that are derived from them.

Ring width or ring area profile models are rare ([10, 13, 26]). Annual ring width profile can be also calculated by the difference between two successive annual inside bark stem profiles [39, 52]. Yet this last method, albeit more widespread, is open to criticism because a static model (stem profile) is being used to generate dynamic increment data: this method is not 'compatible', in the sense defined by Clutter [8] for stand growth models.

The amount of bark, which varies greatly from one species to another, is often modelled using a bark factor (i.e. the ratio diameter inside bark/diameter outside bark) [7, 20, 31, 60]. Despite a few exceptions [40, 60], this ratio rarely remains constant all along the stem. In the models, it often depends on the level in the tree [23, 31].

Although there is a wide variety of models used for predicting the amount of sapwood at a particular height (1.30 m or at the crown base level) [11, 30, 61], there are few models which take into consideration the height in the tree (i.e. the vertical position along the stem). Gjerdrum [21] predicted the number of heartwood rings from the total number of rings using a simple linear relationship, at any height on the tree. Starting at the first appearance of heartwood in the top of the tree and descending to the base, the number of sapwood rings was found to increase while the sapwood width remained constant for trees of similar age [63]. However, according to Dhôte et al. [15], the sapwood ring number remained stable between 10 and 70% of the tree height for oak trees which have grown under a variety of conditions. Other authors have applied models normally used for the stem profile to the sapwood profile [32, 46]. With the exception of those which predict the sapwood or heartwood ring number in relation to the total number of rings in a section, these models do have one major inconvenience in that they are not always compatible with the stem profiles. For example, they may generate incoherent values such as a proportion of sapwood of over 100% at some levels of the tree.

This brief review also shows that only a few studies (e.g. [15]) have attempted to propose a set of stem, ring, bark, sapwood profile models which are compatible with each other along tree growth.

2. MATERIALS AND METHODS

2.1. Data acquisition

A total of 79 cedar trees were selected from 18 even-aged stands in the south-east of France in which temporary or semi-permanent plots had been set up to be monitored regularly. Four trees each were sampled from 11 stands, 2 from 4 other stands, 7 from another, and finally 10 from the remaining two. The trees were chosen so as to cover the range of diameters present in the stand.

The following measurements were taken for each standing tree (*table I*): total height H (in m), diameter at 1.30 m D (in m), height of the base of the first live whorl Hlw (in m), this whorl being defined as the first whorl from the ground with at least one living branch inserted into each of the four quarters of the circumference. The

crown ratio CR (%) was defined as the relative living crown length: $CR = 100 \dfrac{H - Hlw}{H}$.

After felling the trees, the circumference outside bark was measured at each growth unit and at the stump level avoiding any deformations due to the branches. These measurements were used to model the outside bark stem profiles.

Tree discs were sampled from 36 out of the 79 trees (*table I*). The 9 stands from which they came had been chosen for being as different as possible in terms of age, density and productivity. All the discs were used for the bark model. But only 30 out of the 36 trees, representing 8 stands (i.e. 3 to 5 trees per stand), had developed sufficiently for us to be able to measure the heartwood for a minimum of 5 discs per tree: these trees were used to calibrate the sapwood profile model. In total, 1137 tree discs were used for the bark thickness model and 1095 for the sapwood ratio model.

The discs were sampled as follows:

– one disc at the stump,

– between the stump and 1.30 m: one disc approximately every 30 cm,

– one disc at 1.30 m,

– between 1.30 m and the lowest green branch: one disc every three annual growth units,

– between the lowest green branch and the top: one disc per growth unit.

The discs were sampled from a branchless area, between two adjacent whorls. The circumferences of the discs were measured in their fresh state to the nearest millimetre, firstly outside bark then, following debarking, inside bark. The radius of the disc and the radius of the heartwood (delineated by color) were measured in their fresh state to the nearest millimetre in 8 equally distributed directions. The heartwood area of a disc was calculated using the quadratic mean of the heartwood radii. The number of heartwood rings was counted for each radius. As noted, by Polge [48], the heartwood-sapwood boundary often corresponded to an annual ring boundary.

Thirty-two of the 36 trees cut into discs were used in a previous research work to build the ring area profile model [10]. The 4 remaining trees from the same stand in the Luberon region were used to jointly test the stem and ring profile models (*table I*). The discs of the 36 trees were prepared and the ring widths were measured with the same method [10]: After drying, sanding down of the discs and scanning, the ring widths were measured semi-automatically using MacDENDRO™ software [25]

Table I. Main tree measurements of the sample trees. The summary statistics on the left side of the table concern the 79 trees used for the stem profile measurements (first line), the 36 trees used for bark measurements (second line) and the 30 trees used for the heartwood measurements (third line). The main characteristics of the 4 trees used to evaluate the stem and ring profile models are on the right side of the table.

Tree measurement variable	Mean	Standard deviation	Minimum	Maximum	Characteristics of the 4 trees used to test stem and ring profiles			
					1	2	3	4
Age (years)	59	36	20	135	61	61	61	61
	55	26	20	95				
	61	24	27	95				
D (cm)	25.1	16.4	3.5	71.9	16	18	24	28
	23.9	17.7	4.0	71.9				
	26.9	17.9	6.7	71.9				
H (m)	14.54	8.21	3.46	36.10	12.7	13.7	14.6	15.9
	14.63	9.42	3.46	36.10				
	16.36	9.39	4.46	36.10				
H/D (m/m)	64.0	16.7	28.3	120.7	82.3	73.1	62.8	56.8
	67.1	17.4	37.7	120.7				
	65.5	15.6	37.7	102.6				
Hlw (m)	7.73	6.30	0.41	23.55	9.7	9.7	9.9	11.1
	8.43	7.04	0.41	23.55				
	9.79	6.92	0.41	23.55				
CR (%)	54	21	18	96	24	29	32	30
	53	24	19	96				
	48	20	19	96				

accurate to the nearest 0.02 mm. The ring widths were then corrected using the shrinkage values for each radius, whose length had been measured in the fresh state and then dry state, in order to obtain the fresh state values. These data made it possible to calculate the annual ring width profiles and, by accumulating them, the annual inside bark stem profiles.

2.2. Model forms

Generally speaking, for each model, we sought simple formulations with few parameters whose effect on the geometric shape was obvious, so as to be suitable for other coniferous species provided simple reparameterisation is undertaken. We paid attention to the logical behavior of the models and their compatibility with each other.

2.2.1. Stem profile model

The total tree height and the diameter value at 1.30 m are assumed to be known a priori, whether measured or estimated using a model. They are therefore points through which the predicted profile must pass. Two models were chosen: a variable exponent model which had generally given good results in previous studies (cf. 1.2) and a new model we develop here.

Variable exponent model (model I):

The profile of a tree can be described using the simple function: $d(h) = p(H - h)^n$ where H is the total tree height and d is the diameter of the tree at height h, with n and p as positive parameters. If $n = 1$, we are dealing with a cone, when $n < 1$ with a paraboloid, and when $n > 1$ with a neiloid. In a real profile, n varies along the stem: the butt usually resembles a neiloid trunk, the apex

resembles a cone and the intermediate part resembles a paraboloid trunk. Ormerod [47] proposed the following formulation:

$$\frac{d(h)}{d_I} = \left(\frac{H-h}{H-I}\right)^k \qquad (1)$$

where I is any point in the profile $(0 < I < H)$ and $d_I = d(I)$. We chose $I = 1.30$ m. This model satisfies the following condition: $d(h) = 0$. k can be calculated at any point:

$$k = \frac{\ln(d(h)/d_I)}{\ln((H-h)/(H-I))}. \qquad (2)$$

We used for k in equation (1), the following relationship, previously obtained for common spruce [26, 52]:

$$k = a_1 + a_2\left(\frac{h}{H}-1\right) + a_3\,\exp\left(-\frac{a_4}{a_3}\frac{h}{H}\right) \qquad (3)$$

where a_1, a_2, a_3 and a_4 are parameters.

Model II:

This model combines a negative exponential function, which takes into consideration tree form apart from the butt, and a power function which takes into consideration the shape of the basal part.

$$\frac{d(h)}{d_{1.30}} = b_1\left(1 - \exp\left(-\frac{rx^{b2}}{b_3}\right)\right) + b_4\,rx^{b5} \qquad (4)$$

where $rx = \dfrac{H-h}{H-1.30}$, b_1, b_2, b_3 and b_5 are positive parameters, and $b_4 = 1 - b_1\left(1 - \exp\left(\dfrac{-1}{b_3}\right)\right)$ in order to verify $d(h) = d_{1.30}$ when $h = 1.30$ m.

2.2.2. Ring profile model

We used the following trisegmented ring area profile model previously developed and fitted on an independent data set of 32 Atlas cedars [10]. If x is the distance from the tree apex $(= H - h)$, and y the cross-sectional area of the annual ring:

* if $Hlw > 1.30$ m, the model is trisegmented with two join points x_1 and x_2
  – if $x \le x_1$: $y = a(xx_0 - x^2)^b$ $\qquad$ (5.a)
  – if $x_1 < x \le x_2$: $y = cx + d$ $\qquad$ (5.b)
  – if $x_2 < x \le H$: $y = \dfrac{g}{\cos\left(e + \dfrac{x - x_2}{H - x_2}\right)}$ $\qquad$ (5.c)

* if $Hlw \le 1.30$ m then the model becomes bisegmented with only one join point at $x_1 = x_2$. The second segment (Eq. (5.b)) is no longer necessary.

$a, b, c, d, e, f, x_0, x_1, x_2$ are parameters. The continuity constraints of the function and of its derivatives, and forcing function to pass through the point located at 1.30 m, result in dependence between parameters [10].

In order to use the ring profile model for the retrospective modelling of the annual stem and ring profiles, it is necessary to know beforehand the former total height, circumference at 1.30 m and basal area increment, which are obtained by stem analysis. The evolution of the crown base had to be reconstructed. In the absence of any dynamic data concerning the crown recession, a model was therefore established on the basis of 1771 point observations of this variable in a whole range of stands where sample trees, not pruned artificially, were measured (semi-permanent plots and experimental designs). For this purpose we used the model of Dyer and Burkhart [16] which associates the proportion of green crown with available data (age and the corrected slenderness ratio $(H - 1.30)/D$).

$$Hlw = H\,\exp\left[-\left(d_1 + \frac{d_2}{A}\right)\frac{D}{H-1.30}\right] \qquad (6)$$

where A is the age in years, and d_1 and d_2 are parameters.

2.2.3. Bark profile model

In order to obtain the stem profile or increment profile inside bark from the outside bark stem profile, we chose to model the relationship between the outside bark diameter and the inside bark diameter as a function of the distance from the apex. The following model was tested:

$$\frac{D_{out}}{D_{in}} = c_1 + \frac{c_2}{x^{c_3}} \qquad (7)$$

where x is the distance from the apex, D_{out} is the diameter outside bark at x, D_{in} is the diameter inside bark at x, and c_1, c_2, c_3 are positive parameters.

2.2.4. Sapwood profile model

The sapwood thickness value at 1.30 m is assumed to be unknown a priori. We have therefore dismissed the models restricted by this particular value (for example [50]). The evolution of absolute and relative values for width, area and number of sapwood and heartwood rings along the stem was examined as a function of the distance from the apex, the number of rings and the size (diameter and surface) of the section. A model was then proposed

with the following restrictions in order to be compatible with the stem profile. The relative values had to be equal to 1 above the point where the heartwood had appeared, and between 0 and 1 below this point.

Although satisfactory results could be obtained for some trees using simple models (constant number of rings or constant sapwood width below the level where the heartwood has formed), they could not be generalized for our samples as a whole. The following segmented model was finally chosen:

$$- \text{ if } x \le x_{\text{h}}: \frac{sa}{iba} = 1 \qquad (8.\text{a})$$

$$- \text{ if } x > x_{\text{h}}: \frac{sa}{iba} = \exp\left(-e_1(x - x_{\text{h}})\right) \qquad (8.\text{b})$$

where sa is the area of the sapwood cross-section, iba is the area of the inside bark cross-section. This model includes two positive parameters, x_{h} which is the distance from the apex to the point where the heartwood appears, and e_1 which regulates the rate at which the negative exponential decreases. This model is continuous at x_{h} but not its derivative.

2.3 Methodology used for model fitting

Except the crown base model for which fitting was performed in one stage, the methodology used was the same for every model. The analysis was performed in three stages:

First stage: for each tree, the dependent variable was fitted with the following formulation:

$$y_{ij} = f(h_{ij}, H_j, \theta_j) + \varepsilon_{ij} \qquad (9)$$

where y_{ij} is the dependent variable at the ith level of the jth tree, h_{ij} is the height to the ith level of the jth tree, H_j is the total height of the jth tree, θ_j denotes the model parameters of the jth tree, and ε_{ij} is the error. The errors were assumed to have a normal and homoscedastic distribution, and to be random and not autocorrelated.

Second stage: relationships were then investigated between the estimated parameters of these individual models θ_j and the tree measurements:

$$\theta_j = g(\Omega_j, \psi) + \mu_j \qquad (10)$$

where Ω_j represents the vector of the whole tree attributes for the jth tree, ψ the general parameters of the model common to all the trees and μ_j the random error term.

Third stage: θ_j was replaced in (9) using equation (10) and the overall model was adjusted (estimate of ψ) with:

$$y_{ij} = f(x_{ij}, \ g(\Omega_j, \psi)) + \varepsilon_{ij}. \qquad (11)$$

Linear adjustment was performed using the PROC REG procedure, and nonlinear adjustment with the PROC NLIN procedure and the iterative algorithm of Marquardt [35], provided by the SAS/STAT software [53].

2.4 Model evaluation

For most models, basic analysis of model bias and precision was based on the data used to fit them (for the ring profile model it had already been carried out in [10]): examination of usual statistics (*RMSE* = root mean square error, asymptotic standard error of the parameters); examination of the behavior of the residuals (absolute difference between the observed value and the predicted value) and the errors (absolute values of the residuals) in order to detect bias and errors in relation to relative height and tree characteristics; examination of the studentized residuals (ratio of the residual to its standard error) to check regression assumptions (homogeneous variance and normality).

In addition, for stem and ring profiles models, we used the data coming from an independent dataset of 4 trees measured for validation purposes. There are two alternative methods for predicting stem and ring width profiles: (a) in the "integrated method", the stem profile was first modelled and the ring width profile was then obtained as the difference between successive annual stem profiles; (b) in the "incremental method" the profile of ring width (knowing the stem profile, ring width was easily deducted from ring area) was first modelled and the stem profile was then computed as the cumulative output of ring superimposition. We used these two approaches and cross compared them with the aim to test their ability to simulate static stem forms as well as increment profiles.

3. RESULTS

3.1. Stem profile models

The relationships between the parameters of the two models I and II and the tree characteristics (adjustment of the relationship) were established with or without the crown base height *Hlw* which is not always available in practice.

Model I:

a_2 and a_4 are constants.

When the crown base is available, we get:

$$a_1 = a_{11} + a_{12}CR + a_{13}\frac{H-130}{D} \text{ (model Ia).}$$

When the crown base is unavailable, we get:

$$a_1 = a_{11} + a_{12}\frac{H-130}{\sqrt{D}} + a_{13}\frac{H-130}{D} \text{ (model Ib)}$$

and $a_3 = a_{31} + a_{32}\dfrac{H-130}{\sqrt{D}} + a_{33}\dfrac{H-130}{D}$ in both cases.

Model II:

b_1, b_3 and therefore b_4 are constants.

$b_2 = b_{21} + b_{22}CR$ when the crown base is available (model IIa);

$b_2 = b_{21} + b_{22}\dfrac{\sqrt{D}}{H}$ when the crown base is unavailable (model IIb)

and $b_5 = b_{51}H$ in both cases.

The estimated parameters of both general models are given in *table II*. At the individual-tree level, model II proves to be appreciably more accurate than model I (*table III*). Overall, they are similarly accurate but model II has three less parameters. The accuracy of the two models improved when crown base height is available (models Ia and IIa).

We examined the behaviour of the residuals as a function of relative height in the tree (*figure 1*) and the *H/D* ratio (*figure 2*). We calculated, in turn, and by relative height class or by tree, the mean bias and the mean error.

Model II, with or without the crown base, is the model with the lowest bias as a function of relative height. The greatest bias of model II is situated at the base of the tree (*figures 1a and 1b*). However, the two models behave very similarly when the evolution of the mean error along the tree is examined. The error is somewhat autocorrelated along the tree with a maximum at the stump and a minimum above the butt around 1.30 m (*figures 1c and 1d*). This is logical considering the fact that the models were formulated to pass through the value observed at 1.30 m. However, no model appears to generate any marked tendency in relation to the slenderness ratio *H/D* (*figure 2*).

In the remainder of the paper we only kept model II, with or without crown base.

3.2. Crown base height model

The model of Dyer and Burkhart [16] (Eq. (6)) gave satisfactory results. We got: *RMSE* = 1.75 m; *N* = 1771. Values obtained for the parameters, with their asymptotic standard error in parentheses:
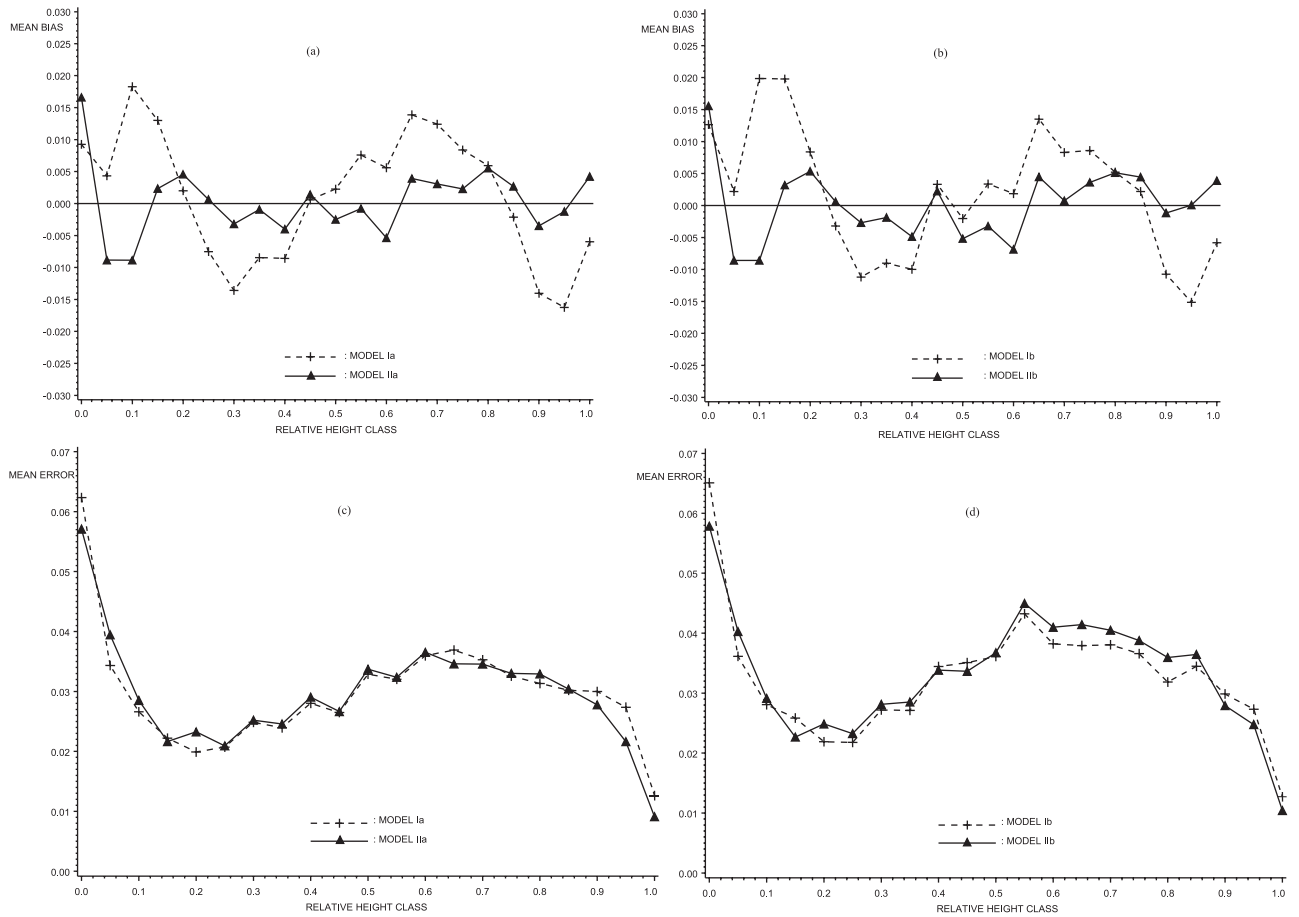
$d_1 = 15.91$ (0.4526)

$d_2 = 881.44$ (25.596).

Table II. Values and standard errors of parameter estimates of the general stem profile model.

Model	Parameters	Model with crown base (a)	Asymptotic standard error	Model without crown base (b)	Asymptotic standard error
I	a_{11}	6.313×10^{-1}	1.704×10^{-2}	1.294	1.470×10^{-2}
I	a_{12}	6.509×10^{-3}	1.731×10^{-4}	-7.913×10^{-3}	3.297×10^{-4}
I	a_{13}	-7.918×10^{-4}	1.877×10^{-4}	-2.772×10^{-3}	2.045×10^{-4}
I	a_2	4.525×10^{-1}	1.535×10^{-2}	4.915×10^{-1}	1.894×10^{-2}
I	a_{31}	1.800	1.069×10^{-1}	1.848	1.104×10^{-1}
I	a_{32}	1.033×10^{-1}	3.577×10^{-3}	9.431×10^{-2}	3.646×10^{-3}
I	a_{33}	-2.802×10^{-2}	2.054×10^{-3}	-2.700×10^{-2}	2.143×10^{-3}
I	a_4	53.049	2.386	43.730	2.124
II	b_1	1.109	1.331×10^{-2}	1.096	1.419×10^{-2}
II	b_{21}	7.524×10^{-1}	1.114×10^{-2}	6.821×10^{-1}	1.460×10^{-2}
II	b_{22}	9.597×10^{-3}	2.203×10^{-4}	15.792	4.517×10^{-1}
II	b_3	5.193×10^{-1}	1.451×10^{-2}	5.066×10^{-1}	1.550×10^{-2}
II	b_{51}	1.392	3.751×10^{-2}	1.351	3.887×10^{-2}

Table III. Accuracy of the estimates using the different stem profile models (2435 observations).

Type of model	Model	Number of parameters	*SSE*	*DF*	*RMSE*
	I	316	0.571152	2119	0.0164
Individual model	II free	395	0.284419	2040	0.0118
	II passing through 1.30 m	316	0.343172	2119	0.0127
General model with crown base	Ia	8	3.891479	2427	0.0400
	IIa	5	3.932583	2430	0.0402
General model without crown base	Ib	8	4.938140	2427	0.0451
	IIb	5	4.840767	2430	0.0446

Figure 1. Mean bias ((a), (b)) and mean error ((c), (d)) of stem profile models as a function of relative height class.

Figure 2. Mean bias ((a), (b)) and mean error ((c), (d)) of stem profile models as a function of slenderness ratio (*H/D*).

3.3. Bark factor model

No relationship was found between the estimated parameters and the tree measurements. The general adjustment (*figure 3* and *table IV*) remained accurate. Residual variance decreases as *x* increases, in contrast to other studies where residual error was higher at the foot of the tree [7, 37]. This is probably due to the difficulty of accurately measuring bark thickness on very small discs. The data were therefore weighted by *x* in order to ensure the equal distribution of studentised residuals (*figure 4*). The values obtained for the parameters, with their asymptotic standard error in parentheses, are the following:

$$c_1 = 1.0532 \ (0.00366)$$

$$c_2 = 0.1580 \ (0.00457)$$

$$c_3 = 0.5656 \ (0.0231).$$

The model has an asymptote at $c_1 > 1$ which guarantees that the model behaves logically ($D_{out} > D_{in}$). The model fits the data observed rather well. The bark factor tends towards infinity when the distance from the apex *x* tends towards 0 but the model yields logical values very quickly ($D_{out}/D_{in} = 2$ for $x = 4$ cm).

3.4. Evaluation of the modelled stem and ring profiles on the independent dataset

3.4.1. Stem profiles

For 4 trees from the same stand in the Luberon region (5329 measurements), we compared the annual stem
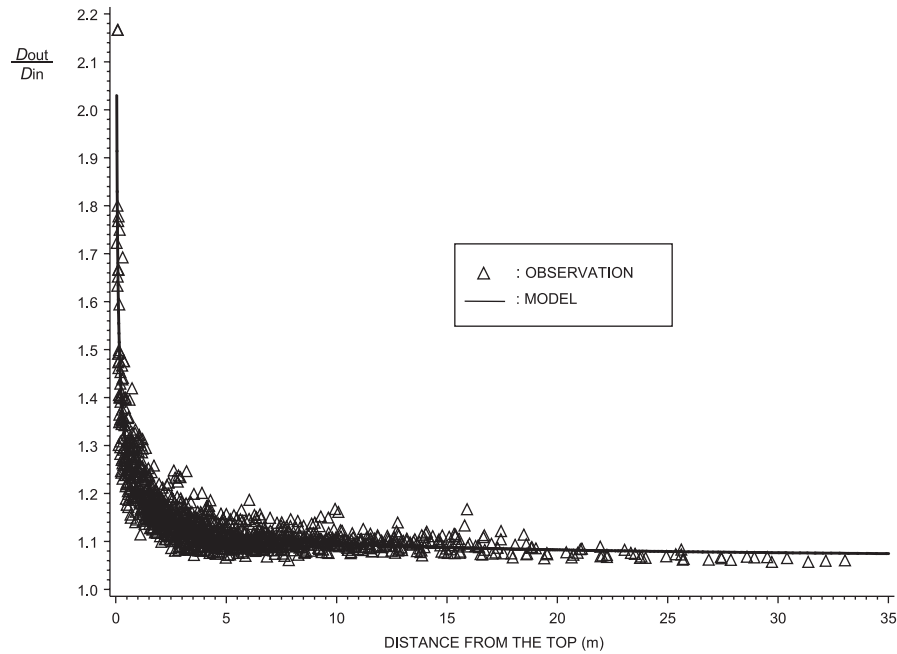
Figure 3. Diameter outside bark/ diameter inside bark ratio (D_{out}/D_{in}) as a fonction of distance from tree top. Observations and fitted general model.

Table IV. Accuracy of estimates using the bark factor model (1137 observations).

Model	Weighted *SSE*	Number of parameters	*DF*	Weighted *RMSE*
Individual model	1.08178	108	1031	0.032424
General model	3.33329	3	1134	0.054216

Table V. Mean bias and error observed when applying different models for predicting the stem profiles of 4 trees from a same stand (5329 observations).

Model used	Mean bias (mm)	Mean error (mm)
Stem profile model with crown base (model IIa)	0.997	2.387
Stem profile model without crown base (model IIb)	1.835	2.976
Ring profile model applied to the estimation of the stem profile	1.783	2.588

profiles measured inside bark with the same profiles modelled via two different approaches:

– integrated approach: we applied the outside bark stem profile model and then the bark factor model to obtain the annual inside bark profiles.
– incremental approach: we cumulatively applied the ring area profile model onto the first basal area stem profile which exceeded a height of 1.30 m.

For the 4 trees measured, the stem profile model IIa with crown base gave the best overall results in terms of bias and accuracy, followed by the ring profile model and then the stem profile model IIb without crown base (*table V*). These results should be modulated according to the part of the tree being dealt with (*figure 5*). At the butt level, the ring profile model gave more accurate, and above all, less biased results than the estimates made by the two stem profile models
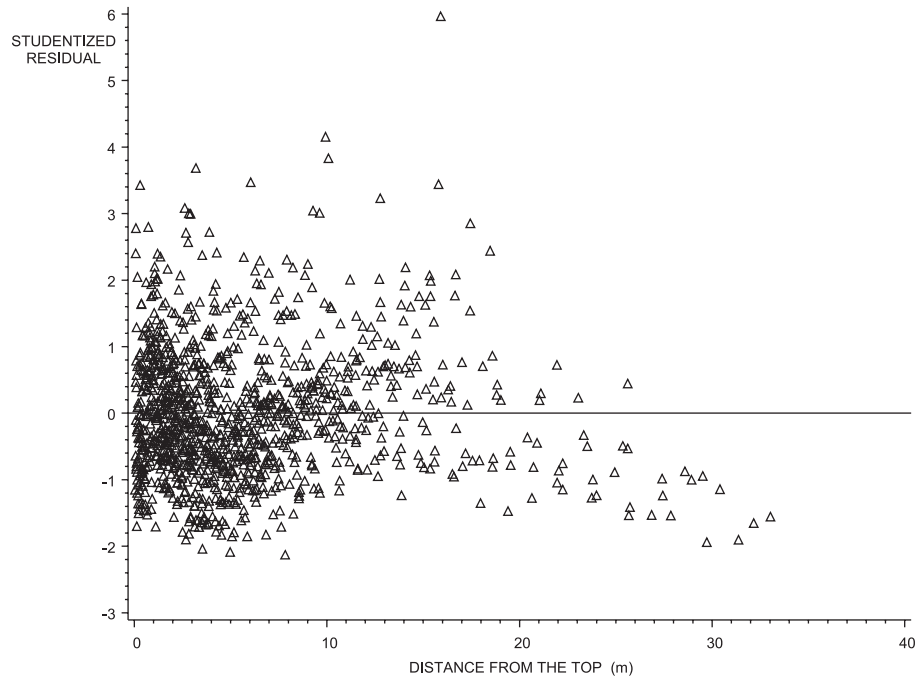
Figure 4. Studentized residuals of the general model of the bark factor (D_{out}/D_{in}) as a function of distance from tree top.
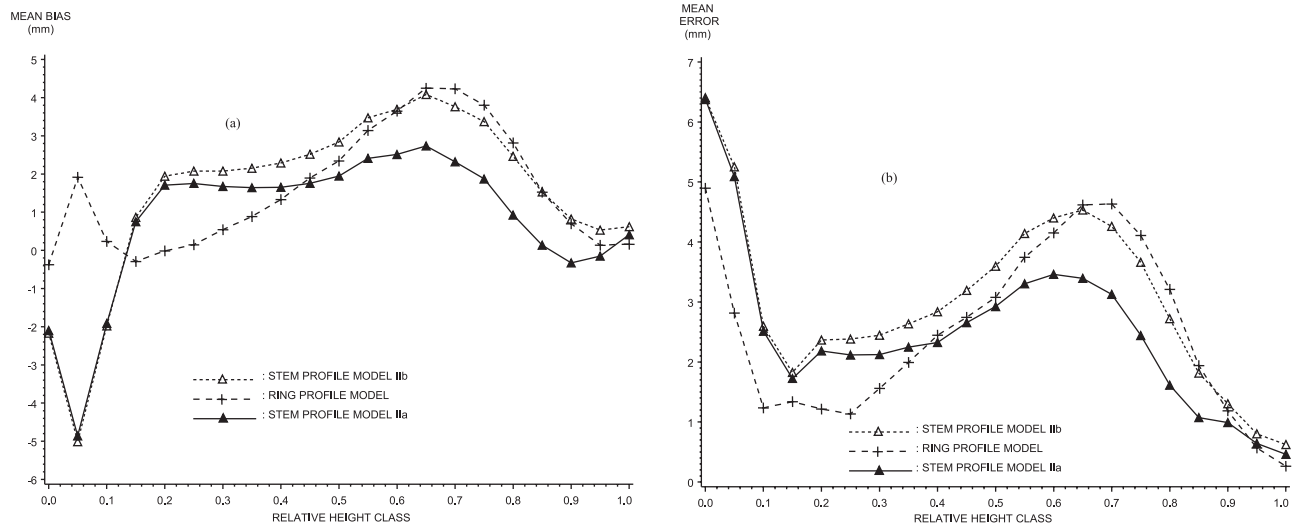

Figure 5. Application of the stem profile models (models IIa and IIb) and ring profile model to all the annual stem profiles of the 4 trees in the Luberon region. Mean bias (a) and mean error (b) as a function of relative height class.

which gave the same results at this level. Moving upwards along the stem, the behaviour of the ring profile model worsens both in terms of bias and accuracy to the point of performing worse at the top of the tree than the stem profile models. Similarly, the stem profile

model without crown base (IIb) becomes more biased and less accurate than the stem profile model with crown base (IIa) and gives mean estimates at this level which are barely better than those of the ring profile model.
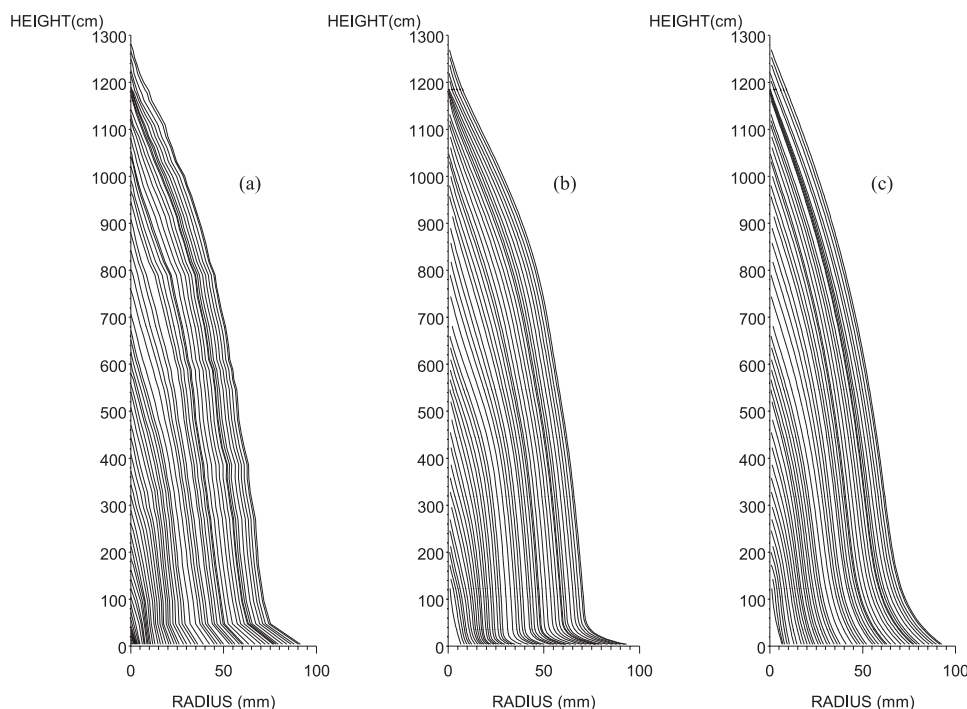
Figure 6. Observed distribution of ring widths for tree 1 in the Luberon region (a), reconstructed by superimposing the rings modelled by the ring profile model (b) and by superimposing the stem profiles modelled by the stem profile model IIa (c).

Table VI. Mean bias and error observed when applying the different models for predicting ring width profiles for 4 trees from a same stand (5329 observations).

Model used	Mean bias (mm)	Mean error (mm)
Stem profile model with crown base (model IIa)	0.070	0.386
Stem profile model without crown base (model IIb)	0.104	0.390
Ring profile model	0.081	0.305

Figure 6 makes it possible to visually compare, for a given tree, the results of the reconstruction of ring distribution using the two methods.

3.4.2. Ring profiles

The measured annual ring width profiles were also compared to the predicted ring profiles obtained by the integrated and the incremental approaches.

The mean performances of the ring area profile model are intermediate between those of the two stem profile models in terms of bias but better in terms of accuracy (*table VI*). The ring profile model is unbiased in the first two thirds along the tree and, conversely, gives the most biased estimates in the upper quarter of the tree. However, it is more accurate for the ring profile as a whole (*figure 7*).

For instance, *figure 8* shows two different rings from the same tree, one of which is predicted more accurately by the ring profile model, the other by the stem profile model.
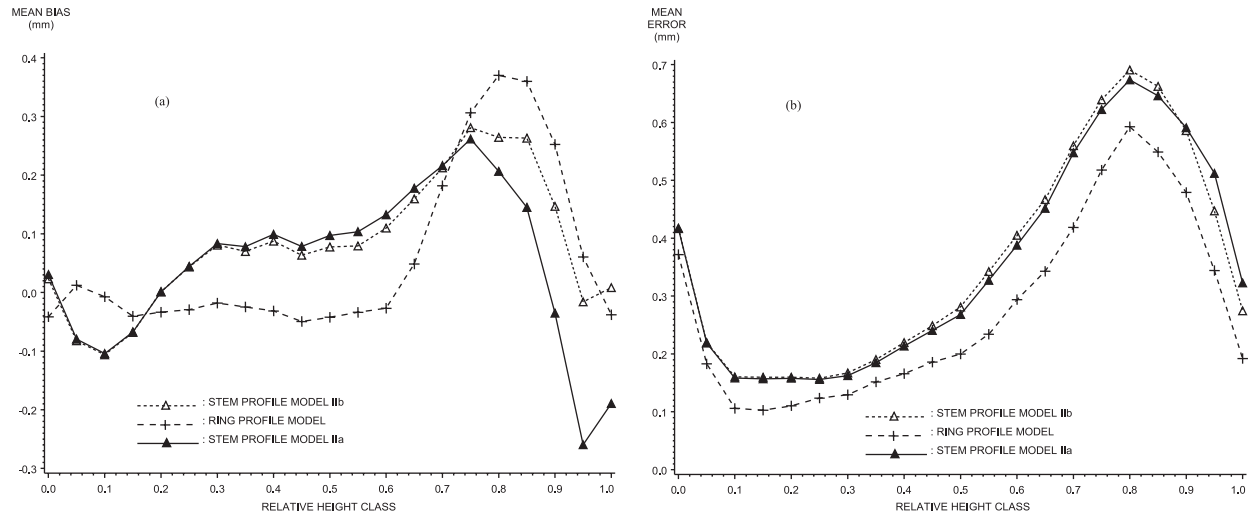
Figure 7. Application of the stem profile model (models IIa and IIb) and the ring profile model to the ring profiles of the 4 trees in the Luberon region. Mean bias (a) and mean error (b) as a fonction of relative height class.
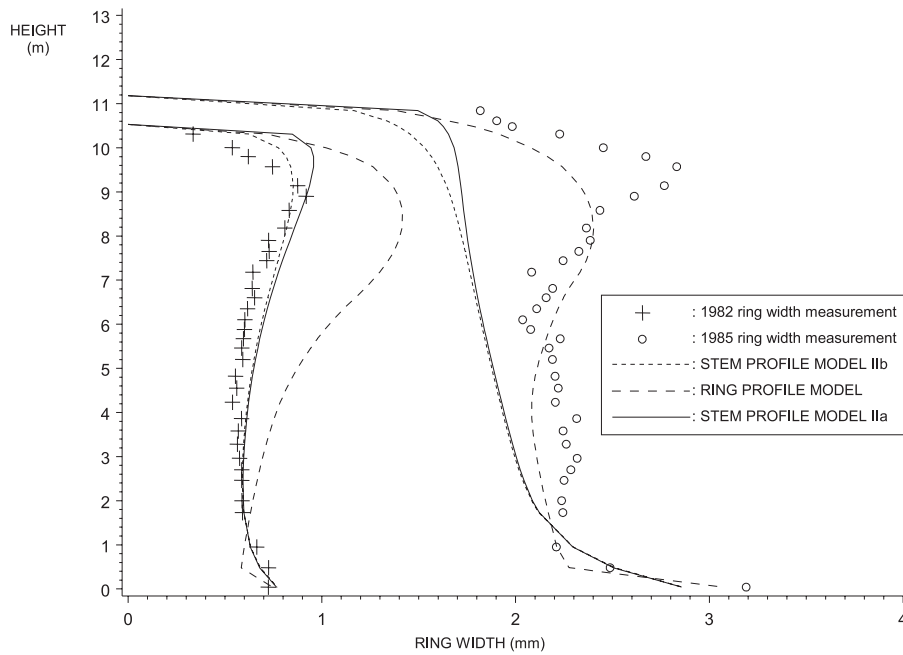

Figure 8. Observed 1982 and 1985 ring width profiles of tree 1 in the Luberon region, and those reconstructed by the difference between successive annual stem profiles (models IIa and IIb) and by the ring profile model.

Table VII. Accuracy of the estimates obtained using the sapwood profile model (1095 observations).

Model	SSE	Number of parameters	DF	RMSE
Individual model	0.286395	2 × 30	1035	0.01663
General model	2.261983	2	1093	0.04549

3.5. Sapwood profile model

An initial individual model was constructed for each tree. Relationships between the two parameters and certain tree characteristics (number of rings, width and area of the sapwood at x_h, tree variables) were then examined. The parameter x_h varied less between trees than the number of rings at the corresponding level (coefficient of variation of 26.9% as opposed to 30.9%). Similarly, variations between trees of parameter b_1 could not be associated with any variable or combination of variables at tree or stand level.

A general model simulating the evolution of the $\frac{sa}{iba}$ ratio was therefore established for all the trees (*figure 9*), even though it was less accurate than the individual model (*table VII*). No bias was observed when we studied the distribution of the residuals according to disc characteristics (mean number and width of the rings of the disc, sapwood area, relative distance from the apex) or tree characteristics (age, dimensions, crown base height).

The values of the parameters, and their asymptotic standard error (in parentheses), of the general model are the following:

$x_h = 4.85$ (0.078) m
$e_1 = 0.0448$ (6 x 10^{-4}) m^{-1}.

4. DISCUSSION

Two stem profile models were tested. They require either the corrected slenderness ratio (($H - 1.30$)/D ratio), or the proportion of live crown. In the absence of artificial pruning of green branches, the two variables are closely related because they both depend on the competition experienced by the tree during growth. The crown base height model confirms that: the nearer the green crown base is to the ground, the more conical the tree and the greater the taper (Eq. (6)). Even so, knowing the crown base height improves the accuracy of stem profile predictions compared to only taking into consideration the slenderness ratio, particularly near the top of the tree,
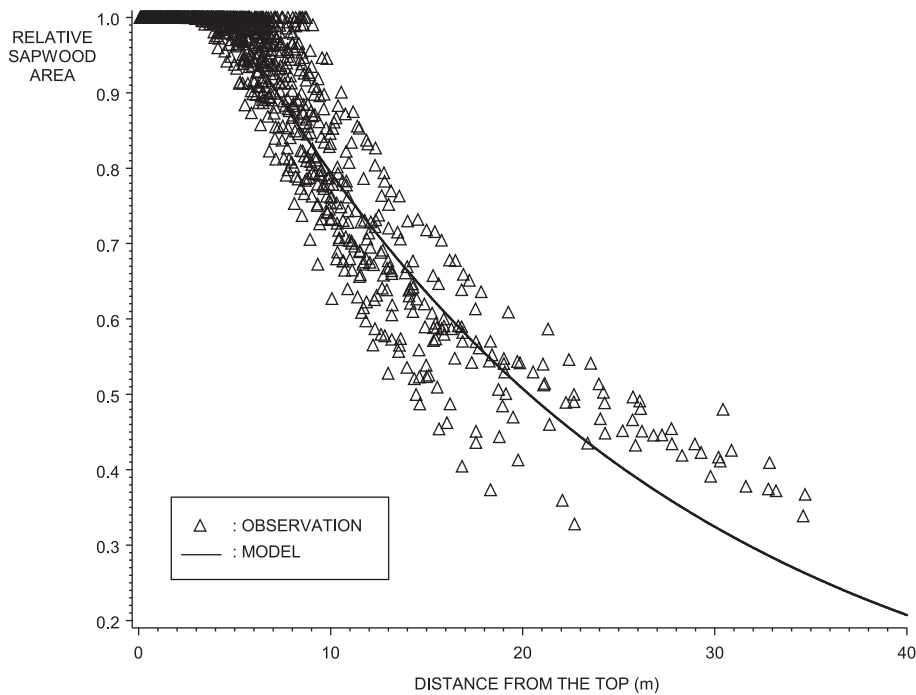

Figure 9. Relative sapwood area as a function of distance from the top. Observations and fitted general model. The value predicted by the model is equal to 1 when the distance from the top is less or equal to 4.85 m.

which coincides with the results of other studies carried out on *Pinus taeda* [5, 41].

The equation which uses the $(H - 1.30)/D$ ratio nonetheless has greater scope because, not only can it be applied to trees for which the diameter and total height are known, but also to artificially pruned trees, since in this case the crown base is no longer that of the crown from which the tree developed. The slenderness ratio, as well as the stem profile, usually integrates tree growth before and, if such is the case, after pruning.

Conversely, it is more logical for the ring profile model to include crown base height since it is an increment model whose profile depends more on the position of the photosynthetic apparatus than on the initial tree form. It is thereby adapted to artificial pruning situations which cause sudden variations in the extent and vertical distribution of annual increment.

The selected stem profile model has only a few parameters. Considering the well-balanced sample, it is well adapted to Atlas cedar. When applied to the 4 independent validation trees, it shows that the bias and error of the estimate are greater at the butt level and that the advantage of using the model with crown base height lies in its greater ability to describe the upper part of the profile. This rather simple model should be tested on other coniferous species. The number of parameters could be reduced even further if b_1 is no longer statistically different from 1.

Although calculating the diameter at a given height poses no problem, it is not possible to analytically compute the height corresponding to a given diameter. Furthermore, this model cannot be integrated analytically to calculate the volume up to any given height or top diameter limit. Nonetheless, approximate calculations by iteration are possible and give perfectly satisfactory results.

It was possible to obtain the annual stem profiles of 4 trees by both the integrated and incremental approaches. Conversely, all the ring width profiles were also predicted using these two approaches. (1) In both cases, the reconstruction of the ring width distributions gives compatible results: the profiles do not intersect and do not generate negative increments. (2) Overall, the ring profile model is more accurate than the stem profile model for predicting ring profiles, whereas the stem profile model is more accurate than the ring profile model for predicting stem profiles. In other words, each profile model proves to be more accurate when used directly to predict the type of profile against which it was calibrated. (3) The accuracy of the models usually differs depending on the part of the tree being dealt with: the ring profile

model gives better results for the butt and the lower part of the stem both for the stem profiles and ring profiles (but poorer results for the upper part of the tree): this model behaviour is interesting in that it is for this part of the trunk that the performance of the stem profile models is the least successful [52], whereas this part is of greatest interest in commercial terms.

The use of static stem profile equations for generating increment values is in theory open to criticism. This method goes hand in hand with the use of derivatives of volume equations for calculating volume increment, whereas they are not intended for this purpose. There is no proof that these volume or profile equations are suitable for describing the evolution of the volume or shape of trees over time. Just as a stand can refer to different volume tables during development, one single profile equation does not necessarily take into consideration the evolution in stem form. For this reason, increment models are, in theory, preferable. This study also shows their superiority when applied in practice.

The models were only tested on 4 trees from the same stand. This test should be repeated on a greater number of trees, particularly trees taken from different stands. Indeed, trees taken from the same plot, regardless of their social status, often have stem profiles or ring profiles which exhibit the same tendencies (e.g. greater or lesser butt) which means that they resemble each other to a greater extent than trees from another stand. Trees are not independent in the statistical sense of the word. Cunia [12] showed that this could result in considerable discrepancies between the biomass measured and the biomass modelled at the stand level, which were in any case much greater than those deduced from the theoretical variances of the model. We therefore come across the same problem here when studying tree form. Another statistical problem, autocorrelation between errors, has not been taken into consideration in this article.

Using the ring profile model improves the bias of the estimates for the tree butt. No doubt because of its segmented formulation, this model seems to be able to take into consideration sudden changes in diameter at this level more easily than stem profile models which generate smoother profiles. Nonetheless, the mean error of the estimates for the butt remains considerable. This part of the tree indeed varies greatly: on the one hand, the diameter varies greatly within a short distance; on the other hand, its form varies greatly between trees. Yet this part of the trunk is the most valuable commercially and is therefore the part which requires greater accuracy when simulating wood quality. Therefore it would be necessary

to sample more trees and also more discs within this part of the tree in order to improve the accuracy of these models, particularly in order to find the segmentation point x_2 which determines the top of the butt in the ring profile model.

For the sapwood area proportion profile, the simple models (constant number of rings or sapwood width below the point where the heartwood has formed) have proved to be inefficient. Their advantage is limited to only a small variety of situations in terms of age and growth conditions [15]. Our sample of 30 stems was noteworthy in that it represented a wide range of silvicultural situations. But it is undoubtedly incomplete and therefore unsuitable for being applied generally. Particularly, we were lacking in data for old trees over 100 years of age.

According to the pipe model theory, the sapwood cross-sectional area, particularly if measured at the crown base rather than at 1.30 m, is a good predictor of leaf area and leaf biomass in trees of different sizes, with more or less developed crowns [4, 33, 45]. Similarly, within a tree, the sapwood cross-sectional area varies from top to bottom of the crown in proportion to the leaf area situated above it [22, 58, 59]. These relationships are not always as simple or as strong as the pipe model predictions. A significant vigour effect is often observed, either directly or via other factors such as climate [3], site index [29], stand density [29, 57, 62] or silvicultural practices [24, 28], either because the functional sapwood often only represents part of the total sapwood or because the specific conductivity of the functional sapwood varies depending on cambial age or social status [17, 54, 55].

The bark factor model was weighted by distance from the apex. This weighting results in greater importance being given to observations at the lower part of the tree, which has the greatest economic value. It is also the part which is most subjected to harmful effects in the case of a fire, whether prescribed or not, and against which the bark has a protective role [51].

The aim of obtaining a coherent set of allometric relationships which describe the internal structure of a trunk has been reached. The models proposed can easily be connected to the outputs of an individual tree growth model which would predict the diameter and height of each tree. The models are compatible and have been formulated so as to make them behave logically: the stem and ring profile models pass through the points located at tree tip and at 1.30 m; the bark factor is always above 1; the sapwood area ratio varies between 0 and 1 and is equal to 1 above the level at which the heartwood

forms; the crown base height, varies between 0 and total height H.

These characteristics which are essential in order to determine the lumber yield and the behaviour of processed wood, are not the only features which may be of interest. These models only make it possible to simulate the internal structure of defect free trees. With respect to the stem, it is also useful to know the amount of defect, the pith position (an eccentric pith is often associated with the curve of the trunk) and the grain angle. These features should be stochastically modeled, because we do not know what determines them.

Branching is also largely responsible for the heterogeneity of the material because of the extent and shape of the knots. A large number of studies have established the determining influence of growth conditions on these characteristics [9, 34, 38]. The internal trunk structure should therefore also be completed by taking into consideration other aspects, in particular branching.

The proposed models are probably valid for Lebanon cedar (*Cedrus libani* A. Richard), which is very common in Turkey and has a similar form. According to Quezel [49], this species and the Atlas cedar are one and the same. The form of the models proposed should be suitable also for a good number of other coniferous species provided that reparameterisation is undertaken.

5. CONCLUSION

This study updates the situation regarding the modelling of the form and internal structure of trunks, by proposing a series of allometric models which are compatible in terms of stem, ring, bark and sapwood profiles. Some models (ring and sapwood profiles in particular) should be validated or reparameterised on more substantial samples so that they can be used more widely.

These data, together with the way they are synthesised in model form, make it possible to increase our knowledge on the way in which a tree develops and functions.

The relationships obtained are to be connected to outputs of a future tree growth model, so as to simulate the form and internal structure of the stems. The different profiles provided here can be predicted from simple and standard tree measurements: total height, diameter at 1.30 m, and if needed the height of the live crown base.

REFERENCES

[1] Bariteau M., Courbet F., Dreyfus Ph., Ducrey M., Du Merle P., Fady B., Oswald H., Teissier du Cros E., Faut-il boiser en région méditerranéenne ?, Forêt-entreprise 93 (1993) 24–45.

[2] Bergqvist G., Wood density traits in Norway spruce understorey: effects of growth rate and birch shelterwood density, Ann. Sci. For. 55 (1998) 809–821.

[3] Berniger F., Nikinmaa E., Foliage area – sapwood area relationships of Scots pine (*Pinus sylvestris*) trees in different climates, Can. J. For. Res. 24 (1994) 2263–2268.

[4] Blanche C.A., Hodges J.D., Nebeker T.E., A leaf area – sapwood area ratio developed to rate loblolly pine tree vigor, Can. J. For. Res. 15 (1985) 1181–1184.

[5] Burkhart H.E., Walton S.B., Incorporating crown ratio into taper equations for loblolly pine trees, For. Sci. 31 (1985) 478–484.

[6] Cao Q.V., Burkhart H.E., Max T.A., Evaluation of two methods for cubic-volume prediction of loblolly pine to any merchantable limit, For. Sci. 26 (1980) 71–80.

[7] Cao Q.V., Pepper W.D., Predicting inside bark diameter for shortleaf, loblolly, and longleaf pines, South. J. Appl. For. 10 (1986) 220–224.

[8] Clutter J.L., Compatible growth and yield models for loblolly pine, For. Sci. 9 (1963) 354–371.

[9] Colin F., Houllier, F. Branchiness of Norway spruce in northeastern France: predicting the main crown characteristics from usual tree measurements, Ann. Sci. For. 49 (1992) 511–538.

[10] Courbet F., A three-segmented model for the vertical distribution of annual ring area. Application to *Cedrus atlantica* Manetti, For. Ecol. Manag. 119 (1999) 177–194.

[11] Coyea M.R.., Margolis H.A., Gagnon R.R., A method for reconstructing the development of the sapwood area of balsam fir, Tree Physiol. 6 (1990) 283–291.

[12] Cunia T., On the error of tree biomass regressions: trees selected by cluster sampling and double sampling, in: Estimating tree biomass regressions and their error, Proc. Workshop on tree biomass regression functions and their contribution to the error of forest inventories estimates, May 26–30, 1986, Syracuse, New York, 1986, pp. 49–59.

[13] Deleuze C., Houllier F., Prediction of stem profile of *Picea abies* using a process-based tree growth model, Tree Physiol. 15 (1995) 113–120.

[14] Demaerschalk J.P., Kosak A., The whole-bole system: a conditionned dual-equation system for precise prediction of tree profiles, Can. J. For. Res. 7 (1977) 488–497.

[15] Dhôte J.-F., Hatsch E., Rittié D., Profil de la tige et géométrie de l'aubier chez le Chêne sessile (*Quercus petraea* Liebl), Bull. Techn. ONF 33 (1997) 59–82.

[16] Dyer M.E., Burkhart H.E., Compatible crown ratio and crown height models, Can. J. For. Res. 17 (1987) 572–574.

[17] Ewers F.W., Cruiziat P., Measuring water transport and storage, in: Lassoie J.P., Hinckley T.M (Eds.), Techniques and Approaches in Forest Tree Ecophysiology, CRC Press, Boca Raton, Louisiana, 1991, pp. 91–115.

[18] Fonweban J.N., Houllier F., Tarifs de cubage et fonctions de défilement pour *Eucalyptus saligna* au Cameroun, Ann. Sci. For. 54 (1997) 513–527.

[19] Forslund R.R., The power function as a simple stem profile examination tool, Can. J. For. Res. 21 (1990) 193–198.

[20] Fowler G.W., Damschroder L.J., A red pine bark factor equation for Michigan, North. J. Appl. For. 5(1) (1988) 28–30.

[21] Gjerdrum P., Prediction of heartwood in *Pinus sylvestris*, in: Nepveu G. (Ed), Proc. 3rd Workshop: Connection between silviculture and wood quality through modelling approaches ans simulation software, September 5–12, 1999, La Londe-Les-Maures, 1999, pp. 145–148.

[22] Gilmore D.W., Seymour R.S., Maguire D.A., Foliage – sapwood area relationships for *Abies balsamea* in central Maine, U.S.A, Can. J. For. Res. 26 (1996) 2071–2079.

[23] Gordon A., Estimating bark thickness of *Pinus radiata*, N. Z. J. For. Sci. 13 (1983) 340–353.

[24] Granier A., Etude des relations entre la section du bois d'aubier et la masse foliaire chez le Douglas (*Pseudotsuga menziesii* Mirb. Franco), Ann. Sci. For. 38 (1971) 503–512.

[25] Guay, R., Gagnon, R., Morin, H., A new automatic and interactive tree ring measurement system based on a line scan camera, For. Chron. 68 (1992) 138-141.

[26] Houllier F., Leban J.-M., Colin F., Linking growth modelling to timber quality assessment for Norway spruce, For. Ecol. Manage. 74 (1995) 91-102.

[27] Kozak A., A variable exponent taper equation, Can. J. For. Res. 18 (1988) 1363–1368.

[28] Långström B., Hellqvist C., Effects of differents pruning regimes on growth and sapwood area of Scots pine, For. Ecol. Manag., 44 (1991) 239–254.

[29] Long J.N., Smith F.W., Leaf area – sapwood area relations of lodgepole pine as influenced by stand density and site index, Can. J. For. Res. 18 (1988) 247–250.

[30] Maguire D.A., Hann D.W., The relationship between gross crown dimensions and sapwood area at crown base in Douglas-fir, Can. J. For. Res. 19 (1989) 557-565.

[31] Maguire D.A., Hann D.W., Bark thickness and bark volume in Southern Oregon Douglas-Fir, West. J. Appl. For. 5 (1990) 5–8.

[32] Maguire D.A., Battista J.L.F., Sapwood taper models and implied sapwood volume and foliage profiles for coastal Douglas-fir, Can. J. For. Res. 26 (1996) 849–863.

[33] Mäkelä A., Virtanen K., Nikinmaa E., The effects of ring width, stem position, and stand density on the relationship between foliage biomass ans sapwood area in Scots pine (*Pinus sylvestris*), Can. J. For. Res. 25 (1995) 970–977.

[34] Mäkinen H., Effect of stand density on radial growth of branches of Scots pine in southern and central Finland, Can. J. For. Res. 29 (1999) 1216–1224.

[35] Marquardt, D.W., An algorithm for least squares estimation of non linear parameters, J. Soc. Indust. App. Math. 11 (1963) 431–441.

[36] Max T.A., Burkhart H.E., Segmented Polynomial Regression Applied to Taper Equations, For. Sci. 22 (1976) 283–289.

[37] Meredieu C., Croissance et branchaison du Pin laricio (*Pinus nigra* Arnold *ssp. Laricio* (Poiret) Maire). Elaboration et évaluation d'un système de modèles pour la prévision de caractéristiques des arbres et du bois. Thèse de Doctorat, Université Claude Bernard Lyon I, 1998.

[38] Meredieu C., Colin F., Herve J. C. Modelling branchiness of Corsican pine with mixed-effect models (*Pinus nigra* Arnold ssp. *laricio* (Poiret) Maire), Ann. Sci. For. 55 (1998) 359–374.

[39] Meredieu C., Colin F., Dreyfus Ph., Leban J.-M. A chain of models from tree growth to properties of boards for *Pinus nigra* ssp. *laricio* Arn.: simulation using CAPSIS (c) INRA and WinEpifn (c) INRA. in: Nepveu G. (Ed.), Proceedings of the third workshop: Connection between silviculture and wood quality through modelling approaches ans simulation software, September 5-12, 1999, La Londe-Les-Maures, 1999, pp. 505–513.

[40] Meyer H.A., Bark volume determination in trees, J. For. 44 (1946) 1067–1070.

[41] Muhairwe C.K., LeMay V.M., Kozak A., Effects of adding tree, stand, and site variables to Kozak's variable-exponent taper equation, Can. J. For. Res. 24 (1994) 252–259.

[42] Nepveu G., Blachon J.-L., Largeur de cerne et aptitude à l'usage en structure de quelques conifères: Douglas, Pin sylvestre, Pin maritime, Epicea de Sitka, Epicéa commun, Sapin pectiné. Rev. For. Fr. XLI 6 (1989) 497–506.

[43] Newberry J.D., Burkhart H.E., Variable-form stem profile models for loblolly pine, Can. J. For. Res. 16 (1986) 109–114.

[44] Newnham R.M., Variable-form taper functions for four Alberta tree species, Can. J. For. Res. 22 (1992) 210–223.

[45] O'Hara K.L., Valappil N.I., Sapwood – leaf area prediction equations for multi-aged ponderosa pine stands in western Montana and central Oregon, Can. J. For. Res. 25 (1995) 1553–1557.

[46] Ojansuu R., Maltamo M., Sapwood and heartwood taper in Scots pine stems, Can. J. For. Res. 25 (1995) 1928–1943.

[47] Ormerod D.W., A simple bole model, For. Chron. 49 (1973) 136–138.

[48] Polge H., Influence de la compétition et de la disponibilité en eau sur l'importance de l'aubier du Douglas, Ann. Sci. For. 39 (1982) 379–398.

[49] Quezel P., Cèdres et cédraies du pourtour méditerranéen: signification bioclimatique et phytogéographique, Forêt méditerranéenne XIX 3 (1998) 243–260.

[50] Ryan M.G., Sapwood volume for three subalpine conifers: predictive equations and ecological implications, Can. J. For. Res. 19 (1989) 1397–1401.

[51] Ryan K.C., Rigolot E., Botelho H., Comparative analysis of fire resistance and survival of mediterranean and western north american conifers, in: Proceedings of the 12th Conference on Fire and Forest Meteorology, October 26–28, 1993, Jekyll Island, GA,1994, pp. 701–708.

[52] Saint-André L., Leban J.M., Houllier F., Daquitaine R., Comparaison de deux modèles de profils de tige et validation sur un échantillon indépendant. Application à l'Epicéa commun dans le nord-est de la France. Ann. For. Sci. 56 (1999) 121–132.

[53] SAS Institute Inc., SAS/STAT user's guide, version 6, fourth edition. SAS Institute Inc., Cary, NC, USA, 1990.

[54] Shelburne V.B., Hedden R.L., Effect of stem height, dominance class, and site quality on sapwood permeability in loblolly pine (*Pinus taeda* L.), For. Ecol. Manag. 83 (1996) 163–169.

[55] Shelburne V.B., Hedden R.L., Allen R.M., The effect of site, stand density, ans sapwood permeability on the relationship between leaf area and sapwood area in loblolly pine (*Pinus taeda* L.), For. Ecol. Manag. 58 (1993) 193–209.

[56] Thomas C.E., Parresol B.R., Simple, flexible, trigonometric taper equations., Can. J. For. Res. 21 (1991) 1132–1137.

[57] Thompson D.C., The effect of stand structure and stand density on the leaf area – sapwood area relationship of lodgepole pine, Can. J. For. Res. 19 (1989) 392–396.

[58] Waring R.H., Schoeder P.E., Oren R., Application of the pipe model theory to predict canopy leaf area., Can. J. For. Res. 12 (1982) 556–560.

[59] Whitehead D., Edwards W.R.N., Jarvis P.G., Conducting sapwood area, foliage area, and permeability in mature trees *of Picea sitchensis* and *Pinus contorta*, Can. J. For. Res. 14 (1984) 940–947.

[60] Wiant H.V., Wingerd D.E., Variation of DIB/DOB ratios with height on hardwood trees, West Virginia For. Notes 11 (1984) 19–20.

[61] Yang K.C., Hazenberg G., Sapwood and heartwood width relationship to tree age in *Pinus banksiana*, Can. J. For. Res. 21 (1991) 521–525.

[62] Yang K.C., Hazenberg G., Impact of spacings on sapwood and heartwood thickness in *Picea mariana* (Mill.) B.S.P. and *Picea glauca* (Moench.) Voss, Wood Fiber Sci. 24 (1992) 330–336.

[63] Yang K.C., Hazenberg G., Bradfield G.E., Maze J.R., Vertical variation of sapwood thickness in *Pinus banksiana* Lamb. and *Larix laricina* (Du Roi) K. Koch, Can. J. For. Res. 15 (1985) 822–828.